Electronic structure and molecular geometry of main group halides

Yu.A. Buslaev and A.P. Klyagina
Kurnakov Institute of General and Inorganic Chemistry, Academy of Sciences of Russia, Leninsky Prospect 31, Moscow B-71 GSP-1 117907 (Russia)

(Received 1 June 1992)

CONTENTS

A. INTRODUCTION

Quantum-chemical calculations of the electronic structure and molecular geometry are usually carried out within the molecular orbital (MO) method [1–3]. The commonly accepted concepts of symmetry and topology of canonical MOs underlie most of the qualitative models proposed for the interpretation of bonding, structure, spectral features, reactivity, and many other molecular properties [4–8]. At the same time, molecular shapes are predominantly described using the model of valence shell electron pair repulsion (VSEPR) developed by Gillespie and Nyholm [9]. During the last decade, this model has gained considerable support from experimental studies of electron deformation density [10–12], whose determination and interpretation have been improved [13], and a deep theoretical justification in the study of the Laplacian electronic charge distribution [14,15] as well as other methods of investigating electron density localization [16]. In recent years, the electron deformation density and the Laplacian of the charge density have been used increasingly in the analysis of bonding [17,18].

Among the qualitative approaches developed within the MO model for explain-

* *Correspondence to:* Yu.A. Buslaev, Kurnakov Institute of General and Inorganic Chemistry, Academy of Sciences of Russia, Leninsky Prospect 31, Moscow B-71 GSP-1 117907, Russia.

0010-8545/93/$24.00

ing and predicting molecular shapes, the most widely applied are the Mulliken–Walsh diagram (MWD) techniques [19,20]. In the literature, much attention has been paid to the physical justification of the MWD model, the possibility of replacing the total energy of a system by the sum of orbital energies calculated within various MO approximations, and the use of such other parameters as the MWD ordinate. These works have been cited and analysed in detail in the review by Buenker and Peyerimhoff [7] and in the book by Gimarc [5]. An attempt to represent the quantitative ordinate in the MWD model by molecular-orbital valence was reported in ref. 21.

The equivalence of the MWD and VSEPR models in explaining and predicting molecular shapes was convincingly demonstrated long ago [22,23]. Qualitative analysis of bond length variations which depend on the number of electrons in a system is usually performed in terms of the MO method [7,24,25]. The VSEPR model is quite often the subject of critical remarks such as those found, for example, in ref. 26. Nevertheless, the model still remains [27,28] the principal tool to explain the shapes of non-transition element molecules. At the same time, researchers still attempt [5,6] to develop a similar, simple and efficient, approach to predict molecular shapes within the MO framework. This approach is attractive because it promises a unified description of the electronic structure, properties, and geometry of molecules in both the ground and excited states, and direct comparison between qualitative models and the results of non-empirical calculations.

The successful application of the extended Huckel MO method and quite simple considerations of the variations in the angular overlap between the central atom and ligands, and of ligand–ligand interactions for explaining the shapes of many molecules [5,6] has suggested that there must exist a simple fundamental principle for determining molecular geometry [29–31]. In this respect, a reasonable approach is to use the symmetry and nodal properties of the canonical MOs [31–34]. Studies of changes in the angular overlap and the structure of ligand group orbitals can be treated as a part of the analysis of the nodal properties of MOs, while the determining role should belong to estimating the bonding (or rather antibonding) character of MOs in the bond region between the central atom and ligands [31].

The present review interprets currently available data on molecular shapes and bond lengths of main group halides AX_k within the framework of a qualitative approach based on the analysis of the MO nodal properties. We shall also discuss bonding features which are important for an explanation of the molecular geometry of the compounds considered. In order to reduce the number of references, we cite recent reviews and papers to which the reader should refer for a more complete list of earlier works.

B. PRINCIPLES OF THE DESCRIPTION OF STRUCTURE AND BONDING

As already mentioned above, the analysis of the bonding and molecular properties, including geometrical parameters, will be performed in terms of the canonical

MOs belonging to irreducible representations of the point symmetry group of the molecules considered.

Molecular orbitals are conventionally constructed within the basis set of valence s- and p-type atomic orbitals (AOs), while d-AOs play the role of polarization functions to provide an increase in flexibility of the basis set in calculations. This point of view is quite common [35–49], although attempts have been made to justify the use of d-AOs in qualitative schemes describing molecular shapes and bonding, particularly in systems with excess electrons [47–51], and will also be given some attention below.

The difference in properties between the first (Li–Ne) and higher-row elements is mainly attributed to the fact that the radii of 2s- and 2p-AOs are close to each other while those of *n*s- and *n*p-AOs in elements of other rows are considerably different. Such an analysis has been successfully applied to hydrides AH_k and diatomic molecules A_2 by Kutzelnigg [46]. In ref. 52, the influence of this factor on the shape of molecules and ions A_3^q has been discussed on the basis of ab initio calculations. We shall also trace the role of this factor in determining the difference between fluorides and other halides. The larger coordination numbers in the second and subsequent row compounds compared with those of the first row elements are due mainly to the small size of the latter atoms [38,46]. Relativistic effects are noticeably manifested in the bonding character and properties of the fifth row elements [46,52–56].

Main group halides can mostly be classified as electron-rich, hypervalent [57] compounds possessing a smaller number of valence AOs within the sp-basis set compared with that required for the formation of two-centre two-electron (2e-2c) bonds. The description of bonding and geometry in these molecules has often been given within the model of a three-centre four-electron (4e-3c) bond [57–60]. However, it seems that such a division into the normal (2e-2c) and the hypervalent (4e-3c) bonds hardly reflects the real variety of chemical bonds. Moreover, there are cases where the concept of the 4e-3c bonds being weaker compared with the 2e-2c bonds fails to be valid. For example, the energy of hypervalent bonds in SF_6 is close to the energy of 2e-2c bonds in SF_2 [61,62], while the bond length in SF_6 is even shorter than in SF_2 [63]. For this reason, we suggest that a hypervalent character of such systems should be taken into account using a more flexible approach. The excess of electrons (the number of which is l) relative to the number m of AOs participating in bond formation is characterized by a hypervalence index $\eta = l/m$. Below we shall follow a correlation between η and bond length in a series of halides.

The predominant formation of one or another molecular shape will be assessed using the simplest concept of the MO nodal properties [31] in terms of the non-occupation of maximally antibonding MOs (MAMOs). MAMO is designated as the highest antibonding MO of each irreducible representation which is based on both central atom and ligand AOs in the symmetry group to which the molecule belongs. (A more detailed description is given in Sect. D.) From the several geometrical configurations available for the AX_k system, the one in which all the MOs except

for the MAMOs are occupied will be realized. This rule, with a number of exceptions (SF_2, XeF_2, XeF_4, $TeCl_6$, etc.), is discussed in the special section of this review.

The VSEPR separation of the charge density in the form of the lone pairs is described by the MO method in terms of the Berlin–Bader diagrams [64–66] and reflects pushing the electron density out from the bond region. The efficiency of this process for the canonical MOs can be evaluated through negative overlap between AOs of the central atom and those of ligands. An attempt to use this approach for estimating the stereochemical activity of the lone pairs will be demonstrated below for the $[SbX_5]^{2-}$ (X = F and Cl) anions.

C. PARTICIPATION AND ROLE OF VALENCE SHELL s-, p-, AND d-AOs IN BONDING

Main group atoms in their ground state are known to have valence electrons in their s- and p-orbitals. However, the possible participation of vacant d-AOs of the same shell in bonding has been a subject of extensive discussion [39–51]. The demand to take them into account when describing bonding within the valence method was based on the existence of molecules such as PF_5, SF_6, IF_7, and some other electron-rich compounds. In this case, four valence AOs of the central atom are insufficient for the formation of two-orbital two-electron bonds, and one should resort to the Pauling hybrid orbitals sp^3d^k, although Linus Pauling himself has invoked resonance structures for explaining [47,67] bonding in molecules of this type.

Simple physical considerations concerning the fact that d-AOs are both energetically and spatially distant from s- and p-AOs (see, for example, ref. 46) have always introduced some doubts on the participation of the d-orbitals in bonding in compounds of the main group elements [35–38]. Even semiempirical and original nonempirical calculations (whose results are comprehensively summarized in ref. 35), although noticeably overstating the d-AO populations, showed unambiguously that these populations were still essentially lower than would be required to provide the sp^3d- and sp^3d^2-hybridization in the trigonal bipyramid and octahedron configurations for the PF_5 and SF_6 molecules, respectively. Nevertheless, the description of bonding with the d-AO participation are still included in many serious books [50,51] trying to retain the d-orbitals even in the MO model where it is unnecessary.

As has been convincingly demonstrated in the review by Bochvar et al. [38] for N and P atoms and their compounds, the d-AOs of neither atom participate in bonding but play the role of polarization functions, approximately similar in these two cases. The formation of compounds with larger coordination numbers in the case of phosphorus and differences in some other properties between nitrogen and phosphorus compounds were attributed to their different atomic sizes. As already noted, Kutzelnigg [46] has suggested an even more important reason for compounds of the first row elements to differ in properties from those of the higher row elements, namely a proximity of the radii of 2s- and 2p-AOs and difference of *n*s- and *n*p-AO sizes of subsequent-row elements. These considerations make redundant the application of d-AOs to the description of bonding. However, since attempts are still made

to retain the d-AOs in bonding analysis, geometry, and some other properties [50,51,68–71], we shall briefly discuss some aspects of this problem which have been given insufficient attention in the highly informative reviews of Reed et al. [47,48], where it was considered in detail.

The d-AOs were most often used for an explanation of the acceptor ability of the AX_3 molecules such as PF_3, $SbCl_3$, PR_3, etc. in transition metal complexes and other donor–acceptor systems. However, in recent years, several calculations have convincingly demonstrated [41–43] that the lowest unoccupied MO (LUMO) responsible for the acceptor ability of PX_3 consists predominantly of the phosphorus 3p-AO (for PH_3 and PF_3 see Table 1). Despite an equal participation of the 3d-AOs in the PH_3 and PF_3 LUMOs, these molecules exhibit a considerable difference in acceptor properties. The acceptor ability of PX_3 shows a much better correlation with the LUMO energy [41] and can be characterized [42] without any inclusion of d-AOs.

The hypothesis of "qualitatively necessary" participitation of d-AOs has been proposed [71] for those MOs which lack the other AOs of the central atom, for example, in e_g and t_{2g} MOs of SF_6. Indeed, the inclusion of d-orbitals lowers the energy of these levels, especially that of e_g, and usually restores an agreement with experiment in the cases where the order of levels in the sp-basis set is violated. However, on the one hand, many calculations performed in the last decade for the main group halides using the sp basis set also gave the level order in agreement with experiment [39–45,72]. On the other hand, a larger population of the "qualitatively necessary" d-AOs implied [73] by the hypothesis was not confirmed by the calculations [74] for the SF_5Cl molecule (see Table 2). In that case, the b_1 and b_2 MOs include only $3d_{x^2-y^2}$ and $3d_{xy}$ of the S atom valence AOs respectively, while the a_1 and e orbitals include, in addition to 3d-AOs, the other valence atomic orbitals of sulphur. Nevertheless, the populations of both types d-AO are virtually the same.

Usually the vacant d-AOs involved in calculations are more diffuse than the valence s- and p-AOs. This results in an essential increase in bond overlap populations (see, for example, Table 2), which is often interpreted as a considerable growth of the bond strength [75]. However, this conclusion is hardly valid. It can be more convincingly demonstrated for transition metal dimers of which the $(n+1)$s- and nd-AOs

TABLE 1

Energies and atomic compositions of HOMOs and LUMOs for PX_3. From data in ref. 41

PX_3	MO	ε(eV)	3s	3p	3d	s_L	p_L
PH_3	$5a_1$	−6.08	0.14	0.67		0.16	
	3e	0.88		0.36	0.23	0.30	0.11
PF_3	$8a_1$	−7.90	0.29	0.32	0.01	0.01	0.36
	7e	−1.05		0.44	0.23	0.07	0.26

TABLE 2

3d AO populations (q) and bond overlap populations ($P_{S\text{-}L}$) for SF_5Cl

MO	Valent S AO	q(3d-AO) with basis sets		
		I[a]	II[a]	III[a]
a_1	s,p_z,d_z^2	0.25	0.34	0.33
b_1	$d_{x^2-y^2}$	0.26	0.33	0.32
b_2	d_{xy}	0.13	0.21	0.20
e	$d_{(x,y)z}, p_{x,y}$	0.11	0.20	0.18
$P_{S\text{-}L}$	sp basis	I[a]	II[a]	III[a]
$P_{S-F_{eq}}$	0.13	0.40	0.52	0.54
$P_{S-F_{ax}}$	0.17	0.43	0.53	0.54
$P_{S\text{-}Cl}$	0.11	0.30	0.45	0.49

[a]Using sp basis sets of numerical Hartree–Fock functions supplemented by 3d STO: I, $\zeta_S = 2.0$; II, $\zeta_S = 2.0$, $\zeta_{Cl} = 2.5$; III, $\zeta_S = 2.0$, $\zeta_{Cl} = 2.5$, $\zeta_F = 3.0$. From data given in ref. 74.

(the diffuse and contracted functions, respectively) keep electrons in the ground state of atoms, thus making the choice of functions less arbitrary than in the case of vacant d-AOs of the main group elements. Figure 1 shows the comparative data (taken from ref. 76) for the chromium dimer. The $2s_g$ MO, consisting mostly of 4s AOs, lies higher than MOs composed of 3d-AOs although the overlap integral (S) of the 4s-AOs is an order magnitude greater than those of the 3d-AOs. This example reveals that the bonding properties of MOs are determined not only by the magnitude of S but also by its shape and the electron density position relative to the bond. In the case of AX_k^l compounds of the main group elements, the maxima of the central atom d-AOs used are, as a rule, shifted towards the ligands, which decreases their contribution to bonding, even for large S values. Therefore, the contribution of the central atom d-AOs to bond energy characteristics cannot be judged by the magnitude of S alone.

Note that d-AO participation itself can be overestimated due to insufficiency balanced basis sets [35,36] or to compensation of an incorrect choice of the parameter α in the X_α calculations [72].

There are many examples where not only the order of the levels, but also characteristic variations of the properties and reaction ability, e.g. in the series SF_6, SeF_6, TeF_6 [40], the structural features of IF_7 [44] and SF_5O^- [41], and the molecular geometry of NF_k [77] can be explained quite well using the data calculated within the sp-basis sets. Thus, in the SF_5O^- anions, a difference between the S—O and S—F bond force constants correlates with the overlap populations, $P_{S\text{-}X}$, calculated within the sp-basis set (Table 3). This difference is determined, to a considerable extent, by an increase in the overlap of all AOs of the oxygen atom with the

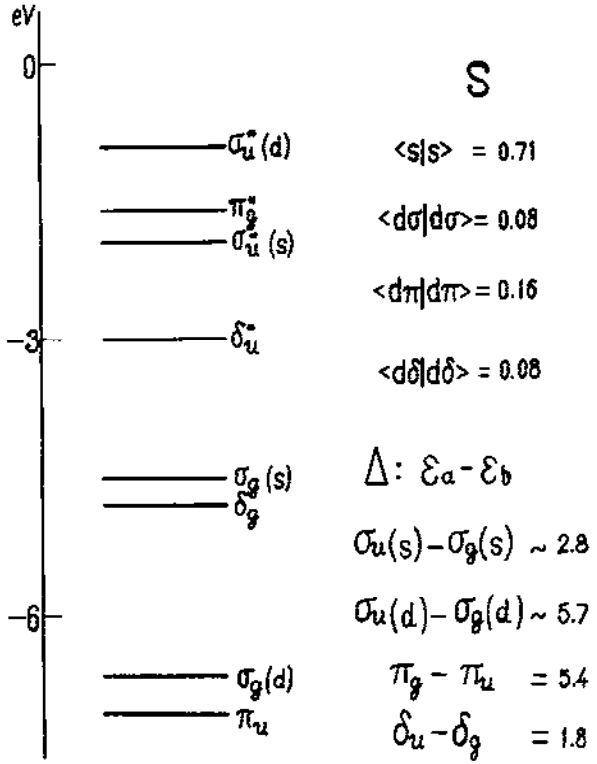

Fig. 1. Energy level diagram, overlap integrals (S) and energy gap (Δ) between bonding and antibonding MOs for Cr_2.

TABLE 3

Bond force constants (k, mdyne $Å^{-1}$), bond overlap populations (P) and AO populations (q) of SF_5O^-

Bond	k	P	Atom	q(2s)	q(2p$_z$)	q(2p$_{x,y}$)
S–O	6.46	0.55	O	1.89	1.19	1.79
S–F_{eq}	3.60	0.08	F_{eq}	1.96	1.51	1.95
S–F_a	3.75	0.10	F_a	1.96	1.50	1.96

corresponding AOs of sulphur compared with that for fluorine (Table 4). Comparison between the populations of the O and F AOs (Table 3) also shows that all the atomic orbitals of oxygen, including 2s, participate in bonding to a greater extent than those of the fluorine atoms. This example also suggests that even the change in atomic orbitals of two neighbouring atoms in the periodic table may produce a considerable effect.

The F 2s- and 2p—AO localisation in roughly the same region of space and

TABLE 4

Overlap integrals of S valent AOs with O and F AOs

AO	2s	2pσ	2pπ	Ligand	R (Å)
3s	0.29	0.31		O	1.47
3p	0.45	0.25	0.23		
3s	0.25	0.27		F	1.47
3p	0.41	0.24	0.20		
3s	0.20	0.24		F	1.60
3p	0.35	0.24	0.16		

the much greater difference in the Cl 3s- and 3p-AOs radii are clearly demonstrated for hexahalide molecules, as indicated by the values of the corresponding overlap integrals (Table 5). This difference seems to be one of the principal reasons for a greater electron affinity for the chlorides compared with the fluorides, due to the less antibonding character of the LUMO in the former case (Table 6). We shall present below some other examples of the influence of this factor in determining some features in the behaviour of fluorides.

Summing up, one may conclude that it is justified and adequate to describe the chemical bonding, structure, and properties of main group compounds using only sp basis sets. For this reason, the subsequent analysis of molecular geometry

TABLE 5

Overlap integrals (S) × 10^3 of some valent AOs: s_A, s_X, p_X in AX_6 [39]

AO	P–X	S–X	Se–X	Te–X	Sb–X
s_A–s_F	235	214	187	189	195
s_A–$p\sigma_F$	238	246	217	194	185
s_A–s_{Cl}	189	157	143	160	173
s_A–$p\sigma_{Cl}$	289	268	245	247	249

TABLE 6

AO coefficients in the highest MO of the a_{1g} representation in AX_6^q [39]

AX_6	MO	$c(ns_A)$	$c(ns_X)$	$c(np\sigma_X)$
SeF_6	$7a_{1g}$	0.98	−0.13	−0.43
$SeCl_6$	$9a_{1g}$	0.78	−0.02	−0.43
$SeCl_6^{2-}$	$9a_{1g}$	0.61	−0.02	−0.42
TeF_6	$8a_{1g}$	1.02	−0.17	−0.41
$TeCl_6^{2-}$	$10a_{1g}$	0.72	−0.05	−0.43

and some features in lone pair behaviour will be performed in terms of this sp-picture, with no account of the d-orbitals in the valence shell at all.

D. MOLECULAR SHAPES OF THE MAIN GROUP HALIDES

The possibility of explaining molecular geometry on the basis of MO nodal properties has been studied earlier [24,31]. It was shown [31] that the shapes of a large number of molecules are determined by the principle of non-occupation of the maximally antibonding MOs (MAMOs). MAMO is the highest antibonding MO for each irreducible representation (IRs) which is based on both the central atom and ligand AOs. Table 6 demonstrates that the highest MO of the a_{1g} representation in AF_6 molecules is completely antibonding in the bond region. We prefer not to use the term completely antibonding molecular orbital (CAMO) [31] since bonding interactions in such MOs can exist between ligand AOs. A simple procedure for counting up the number of MAMOs is demonstrated in Table 7 for linear and bent AX_2 molecules. The a_1, b_2 and b_1 IRs of the C_{2v} group for bent AX_2 molecules have MAMO in the MO basis of each IR, while the a_2 IR is based on a non-bonding MO. So we have three MAMOs in bent AX_2 molecules and, according to similar counting, four MAMOs in linear AX_2, since π_u IR is two-fold degenerate. The numbers of MAMOs for other AX_k molecules are given in Table 8.

Table 8 presents data available for the structures of AX_k halides, illustrating the validity of the MAMO non-occupation rule. Bonding, non-bonding, and partly antibonding MOs which are left after exclusion of MAMOs from consideration in

TABLE 7

Number of MAMOs for linear and bent AB_2 molecules

Symmetry	IR[a]	CA AOs[a]	Ligand SOs[a]	No. of MOs[b]	No. of MAMOs[c]
$D_{\infty h}$	σ_g	s	$s_1 + s_2$, $\sigma_1 + \sigma_2$	3	1
	σ_u	p_z	$s_1 - s_2$, $\sigma_1 - \sigma_2$	3	1
	π_u	$p_{x,y}$	$\pi_1 + \pi_2$	2 × 2	1 × 2
	π_g		$\pi_1 - \pi_2$	1 × 2	0
C_{2v}	a_1	s, p_z	$s_1 + s_2$, $\sigma_1 + \sigma_2$, $\pi_1 + \pi_2$	5	1
	b_2	p_x	$s_1 - s_2$, $\sigma_1 - \sigma_2$, $\pi_1 - \pi_2$	4	1
	b_1	p_y	$\pi_1 + \pi_2$	2	1
	a_2		$\pi_1 - \pi_2$	1	0

[a]IR = irreducible representation; CA = central atom; SO = symmetry-adapted linear combination of AOs.

[b]The number of MOs forming the basis of the IR.

[c]The number of MAMOs transforming as the corresponding IR; MAMO is the highest antibonding MO of the specific IR based on both the CA and ligand AOs.

TABLE 8

Molecular shapes obeying the rule of non-occupation of the MAMO

AX_k	No. of VAO	No. of valence electrons	No. of MAMO	Shape, symmetry	Examples[a]
AX_2	12	16	4	Linear, $D_{\infty h}$	BeX_2, BF_2^+, MgX_2, CaY_2, $SrBr_2$, SrI_2
		18	3	Bent, C_{2v}	CL_2, SiL_2, GeL_2, SnX_2, PbX_2, PF_2^+
AX_3	16	24	4	Planar, D_{3h}	BX_3, AlX_3, GaX_3, InY_3, $TlCl_3$, $TlBr_3$, CF_3^+, CCl_3^+
		26	3	Pyramidal, C_{3v}	NF_3, NCl_3, PX_3, AsX_3, SbX_3, BiY_3, InY_3^{2-}, TlY_3^{2-}, $GeCl_3^-$, SnF_3^-, $SnCl_3^-$, PbF_3^-, SL_3^+, SeX_3^+, TeX_3^+
AX_4	20	32	4	Tetrahedral, Td	BeF_4^{2-}, BX_4^-, AlX_4^-, GaX_4^-, InX_4^-, TlY_4^-, CX_4, SiX_4, GeX_4, SnX_4, PbX_4, NF_4^+, NCl_4^+, PL_4^+, AsX_4^+, $SbCl_4^+$
		34	3	C_{2v}	SF_4, SeF_4, TeF_4, $TeCl_4$, PF_4^-, PBr_4^-, AsL_4^-, SbX_4^-, BiY_4^-, ClF_4^+, BrF_4^+, IF_4^+
AX_5	24	40	4	TBP, D_{3h}	SiF_5^-, GeF_5^-, $SiCl_5^-$, $GeCl_5^-$, $SnCl_5^-$, $SnBr_5^-$, PF_5, PCl_5, AsF_5, $AsCl_5$, SbF_5, $SbCl_5$, $InCl_5^{2-}$, $TlCl_5^{2-}$
		42	3	TP, C_{4v}	SbF_5^{2-}, $SbCl_5^{2-}$, SbI_5^{2-}, $BiCl_5^{2-}$, SF_5^-, SeF_5^-, $SeCl_5^-$, TeF_5^-, $TeCl_5^-$, ClF_5, BrF_5, IF_5, XeF_5^+
AX_6	28	48	4	Octahedral, O_h	AlF_6^{3-}, $InCl_6^{3-}$, $TlCl_6^{3-}$, SiF_6^{2-}, GeF_6^{2-}, $GeCl_6^{2-}$, SnX_6^{2-}, PbF_6^{2-}, $PbCl_6^{2-}$, PF_6^-, PCl_6^-, AsF_6^-, $AsCl_6^-$, SbL_6^-, BiF_6^-, SF_6, TeF_6, ClF_6^+, BrF_6^+, IF_6^+, PoF_6
		50	3	C_{nv}	XeF_6, IF_6^-, $BiBr_6^{3-}$, SbY_6^{3-}, $TeBr_6^{2-}$

[a] X = F, Cl, Br, I; L = F, Cl, Br; Y = Cl, Br, I. From data cited in refs. 5, 28, 63 and 91 and the references cited in Tables 10–12.

systems AX_2^g of $D_{\infty h}$ symmetry may accommodate only 16 electrons while in the bent configuration the $5a_1$, $4b_2$, $2b_1$ MAMOs will remain unoccupied upon arrangement of 18 electrons (see Fig. 2 as a visual aid scheme and here and in what follows, Table 8). A series of AX_3^g compounds clearly shows the pyramidal structure (C_{3v}) to

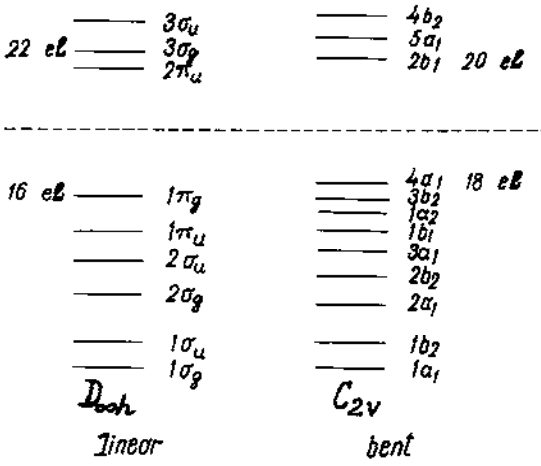

Fig. 2. MO order diagrams for linear and bent AX_2. Here (and in Figs. 4–6) MAMOs are above the broken line.

be more favourable than the planar structure (D_{3h}) for compounds with 25 and 26 electrons because these molecular shapes have three and four MAMOs, respectively (Fig. 3).

The preferable configuration for accommodation of 32 electrons in the AX_4^n systems is tetrahedral (Fig. 4), although its advantage over the square (D_{4h}) is due

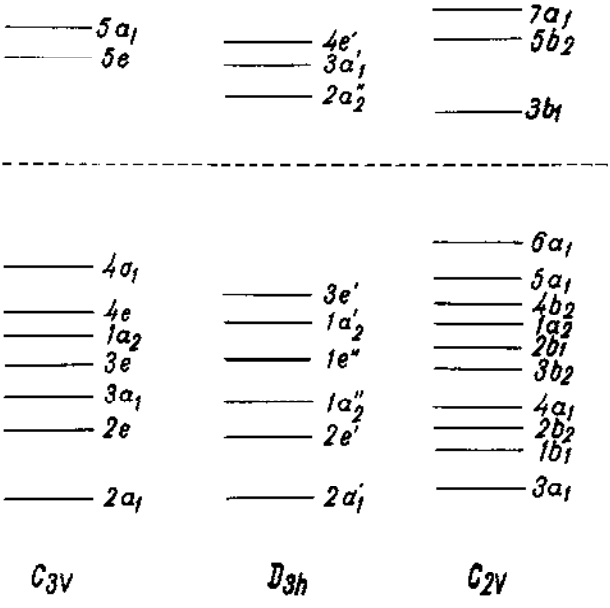

Fig. 3. MO order diagrams for pyramidal (C_{3v}), planar (D_{3h}) and T-shaped (C_{2v}) AX_3.

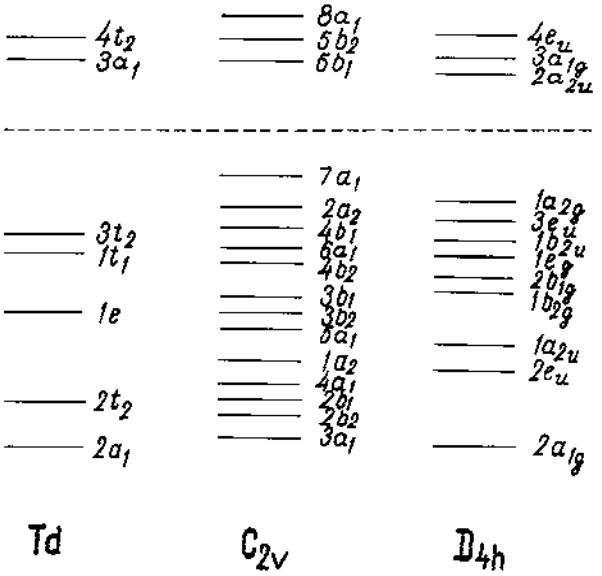

Fig. 4. MO order diagrams for tetrahedral (Td), SF_4 type-shaped (C_{2v}) and square planar (D_{4h}) AX_4.

to more subtle effects than ones considered by the MAMO non-occupation rule. When going to the 34 electron systems, two additional electrons should occupy the MAMO in the tetrahedral structure, while all MAMOs remain unoccupied in the C_{2v} configuration. For the AX_5^ξ systems, the MAMO non-occupation condition is fulfilled in a trigonal bipyramid configuration for 40 electrons, and in the tetragonal pyramid for 42 electrons (Fig. 5).

The MAMOs are unoccupied in AX_6^p compounds with 48 electrons in octahedral configuration, but further addition of electrons would enforce filling these orbitals. At the same time, any C_{nv} structure has one MAMO lacking compared with the octahedral structure. Indeed, AX_6^p compounds with 50 electrons are reported in which a distorted octahedral structure has been observed [78,79]. These examples are given in Table 8.

Table 9 presents some exceptions from the MAMO non-occupation rule. However, in AX_2^ξ and AX_3^ξ systems with 20 and 28 electrons, respectively (Figs. 2 and 3), the MAMOs are π^*-type orbitals ($2b_1$ and $3b_1$, respectively) and they exhibit somewhat less antibonding character compared with σ^*-type MOs. In linear AX_3^ξ compounds with 22 electrons and octahedral AX_6^ξ componds with 50 electrons, the HOMOs include only s-AOs from the central atom basis set contracted to a greater extent compared with the central atom p-AOs, and hence are less antibonding MAMOs than other MAMOs. The two HOMOs in a square structure with 36 electrons (Fig. 4) are MAMOs of the π^*- and "s*"-type, while the MAMOs to be occupied in tetrahedral and C_{2v} structures also include σ^*-type contributions.

An explanation for exceptions from the MAMO non-occupation rule presented

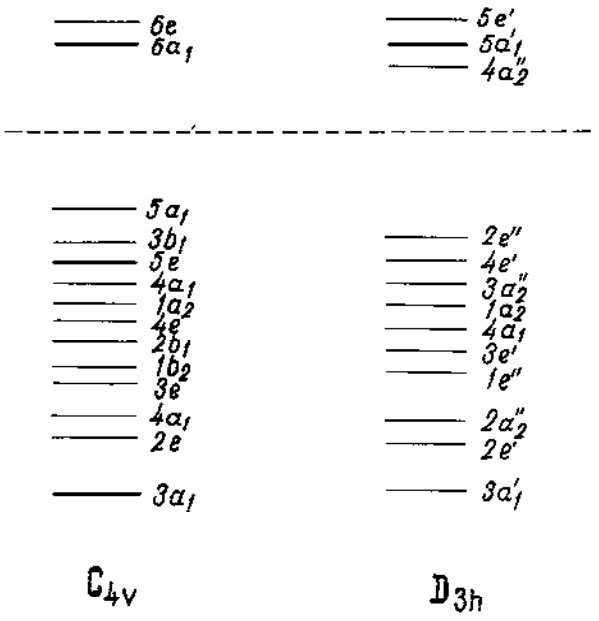

Fig. 5. MO order diagrams for trigonal bipyramidal (D_{3h}) and square pyramidal (C_{4v}) AX_5.

TABLE 9

Exceptions from rule of non-occupation of maximally antibonding MO

AX_k	No. of VAO	No. of valence electrons	Shape, symmetry	Examples[a]
AX_2	12	20	Bent, C_{2v}	OL_2, SF_2, SCl_2, SeL_2, $TeCl_2$, $TeBr_2$, ClF_2^+, BrL_2^+, IY_2^+, Y_3^+
		22	Linear, $D_{\infty h}$	ClF_2^-, $ClBr_2^-$, BrX_2^-, IY_2^-, X_3^-, KrF_2, XeF_2
AX_3	16	28	T-shaped, C_{2v}	ClF_3, BrF_3, $BrCl_3$, SeL_3^-, ICl_3, XeF_3^+
AX_4	20	36	Square planar, D_{4h}	ClF_4^-, BrF_4^-, IF_4^-, ICl_4^-, XeF_4, $SeBr_4^{2-}$, TeY_4^{2-}
AX_6	28	50	Octahedral, O_h	TeY_6^{2-}, SeY_6^{2-}, $SbCl_6^{3-}$, $BiCl_6^{3-}$, ClF_6^-, BrF_6^-

[a] L = F, Cl, Br; X = F, Cl, Br, I; Y = Cl, Br, I. From refs. 5, 28, 63 and 91 and the references cited in Tables 10–12.

in Table 9 may be given as follows. Structures containing occupied MAMOs are those in which the MAMO antibonding character is less pronounced compared with MAMOs of alternative shapes.

Neither the MAMO non-occupation rule nor the VSEPR model can explain the bent geometry of CaF_2, SrF_2, $SrCl_2$, and BaX_2 (X = F, Cl, Br, I) [28,63,80–82] which, according to both these and other applied models must be linear, as is the situation for the remainder of the alkali-earth dihalides (Table 8). This problem has been the subject of much discussion (see, for example, refs. 28 and 82 and the references cited therein).

It has been shown [83] that the inclusion of d orbitals would allow one to explain the bent shape of the above molecules in the framework of the MWD method. Ab initio calculations, with the inclusion of d-AOs in the basis sets, also gave a bent geometry for CaF_2 [82(a),84–87] while within basis sets extended by 4p-AOs, the ground state configuration was linear [84,87]. The potential energy surface was extremely flat for both calculations. The most exact calculations of CaF_2 and $CaCl_2$ [87] within the basis set near the HF limit, with both 3d- and 4p-AOs equally well represented, do not indicate significant bending trends for CaF_2. No qualitative difference from $CaCl_2$ was detected which might explain experimentally observed shapes, i.e. the bent one in CaF_2 and the linear one in $CaCl_2$.

For this reason, the most convincing explanation [87–90] for alkaline earth dihalide structural features seems to be based on the ionic bonding model complemented with a concept of cation polarizability by anions. However, even this suggestion has been called into question [82] in the course of a thorough analysis of multipole expansions describing cation–anion interactions and including terms up to dipole–dipole interactions.

In two recent studies [82(b),(c)], the geometry of alkaline earth dihalides MX_2 (M = Be, Mg, Ca, Sr, Ba; X = F, Cl, Br, I) were obtained from ab initio pseudo-potential calculations at the HF [82(b),(c)] and SDCI [82(c)] levels in agreement with experimental data. It was concluded that both core-polarization and d-AO participation in small covalent bonding contributions control the bending in Ca, Sr, and Ba dihalides. Thus, no simple model is suggested which might adequately describe alkaline earth dihalide geometry.

Radicals and molecules in their excited states can be expected to exhibit shape variations similar to those observed upon filling in the same orbitals in closed shell systems. However, it would be quite natural to suggest that the change in geometry of these species will, as a rule, be less pronounced than that of the closed shell AX_n^k system. Experimental data for AX_n^k systems with unpaired electrons (UE) are few [5,91], but these and results of calculations [92,93] for a sufficiently large number of radicals confirm this suggestion.

These considerations were expressed in the form of a sequence of electron repulsion [92(a)]: LP–BP > BP–BP > UE–BP, within the VSEPR model. In terms of the MO LCAO model, the variation in the electronic structure and its effect on

geometry and stability when going to systems with unpaired electrons was analysed in detail for $PF_5^{2-} \rightarrow PF_5^-$ and $SF_5^- \rightarrow SF_5$ [93(a)], for SF_k^p species ($k = 1-5$, $p = 0, -1$) [93(b)], PX_5^5 (X = F, Cl) [92(b)] and other PCl_k^p ($k = 1-6$) systems [93(c)].

E. CORRELATION BETWEEN BOND LENGTH AND HYPERVALENCE INDEX IN MAIN GROUP HALIDES

The commonly accepted concept of correlation between the bonding character of MO and the bond length (that is, shortening of the latter upon filling up of bonding MOs, its lengthening upon occupation of antibonding MOs, and reverse effects due to electron removal) which was introduced at the onset of quantum-chemical theory is now extensively developed and applied [7,24,25]. It has been shown that such correlations are valid not only in isostructural molecules, but also in systems with different shapes, once it is possible to evaluate and compare the antibonding character of HOMOs in the species studied. Thus, the lengthening of the bonds in the series $XeF_6 < XeF_4 < XeF_2$ can be attributed to an increase in the number of occupied antibonding MOs in this sequence. Also increasing in this series is the antibonding character of the HOMO, which is the main reason for the elongation of bonds in these molecules [5]. A characteristic increase in bond length observed when going from a tetrahedron to a pyramid of C_{3v} symmetry can be related to a change in the antibonding character of the HOMO in the compounds under consideration (see Table 2 in ref. 24).

A simplified version of the MO approach which has been widely used for the description of bonding in hypervalent molecules is represented by the 3-centre 4-electron bonds (4e-3c) model [57–60]. It has especially often been used in explaining the difference between axial and equatorial bond lengths in compounds with trigonal-bipyramid, tetragonal-pyramid, and other structures containing non-equivalent bonds [57,94,95]. The character of this difference is well determined and a sufficiently complete list of examples can be found in Table 12 (see below). As far as we know, the only exception from the regularities established is a longer axial bond compared with equatorial bonds in the tetragonal-pyramid cation of the compound $[XeF_5]^+[AgF_4]^-$ (1.853 vs. 1.826 Å) [96]. This has been attributed to a stronger interaction of the anion fluorine atoms with the cation compared with that in $[XeF_5]^+[MF_6^-]$ and other XeF_5^+ containing compounds [96].

The concept of weaker hypervalent (4e-3c) bonds was used to explain [97] the spontaneous fragmentation $XeF_6 \rightarrow XeF_5^+ + F^-$ and $AX_4 \rightarrow AX_3^+ + X^-$ in the solid state and a failure in attempting to obtain TeF_6^{2-} and SbF_6^{3-} although TeF_5^- and SbF_5^{2-} do exist.

However, as already noted above, the discrimination between 4e-3c and 2e-2c bonds is crude and far from always justified. From Fig. 6, one can see that energies and overlap populations of hypervalent bonds in SF_6 are close to those of two-electron bonds in SF_2, yet the bonds in SF_6 are even shorter than those in SF_2.

For this reason, we suggest a more flexible approach to evaluating the hyperva-

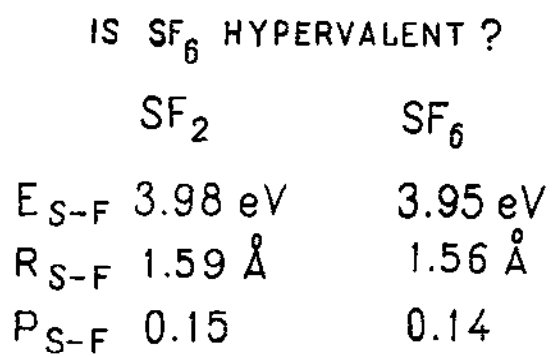

Fig. 6. Comparison of bond energies (E), bond lengths (R) and bond overlap populations (P) for SF_2 and SF_6.

lent character of the AX_k^p systems by introducing a hypervalence index (η) determined as the ratio of the number of electrons (l) to that of the orbitals (m) participating in σ-bonds ($\eta = l/m$). For main group halides, we take into account the valence electrons and four AOs of the central atom, one electron and one orbital for each halogen atom, and the total charge. For example, in SbF_5^{2-}, TeF_5^-, IF_5, and XeF_5^+, we have $\eta = 12/9 = 1.33$, while in CF_4, BF_4^-, and NF_4^+ $\eta = 1$.

The η values and bond lengths for molecules with equivalent bonds are given in Tables 10 and 11 for fluorides and other halides, respectively. These data reveal good correspondence between η and bond lengths in the AX_k^l halide series. The correlation is satisfactory if we take into account a scattering of 0.02–0.03 Å in bond lengths as obtained by different methods (see, for example, Table 20.2 in ref. 63), a decrease in the AO radii along the row, and the fact that AOs become more diffuse when going from cations to neutral molecules and anions. In particular, the larger value of the bond lengths in SF_2 compared with that in SF_6 corresponds quite naturally to the higher η value in the former case (see Fig. 6 and Table 10).

In molecules with trigonal-bipyramid, tetragonal-pyramid, and some other structures (Table 12) containing bonds of different lengths, a correlation between η and bond lengths is observed for each particular bond type. The mean values of these bond lengths also agree with the general pattern if we take into account the factors mentioned above which violate the correlation. Such a correspondence between η and bond lengths is not so surprising if one takes into account the fact that η can be interpreted as an averaged indicator of the antibonding character [24] of the MOs participating in bonding.

In conclusion, note that possible applications of the hypervalence index are not restricted to correlations with geometric parameters. In the following section we shall briefly discuss the applicability of η to describing the behaviour of lone pair electrons. A most interesting example is offered by the possible use of η to assess the direction of chemical transformations for a wide range of compounds, namely of

TABLE 10

Correlation between hypervalence index, η, and bond length (Å). From data in refs. 5, 28, 63 and 91

AX_4, T_d $\eta = 1.00$	AX_3, C_{3v} 1.14	AX_6, O_h 1.20	AX_2, C_{2v} 1.33	AX_6, $\approx O_h$ 1.40	AX_4, D_{4h} 1.50	AX_2, $D_{\infty h}$ 1.66
BF_4^-, 1.41						
CF_4, 1.32	NF_3, 1.37		OF_2, 1.41			
NF_4^+, 1.30						
		PF_6^-, 1.58				
SiF_4, 1.55	PF_3, 1.57	SF_6, 1.56	SF_2, 1.59			
	SeF_3^+, 1.50		ClF_2^+, 1.57			
		GeF_6^{2-}, 1.77				
GeF_4, 1.66	AsF_3, 1.71	AsF_6^-, 1.69				
	SeF_3^+, 1.66	SeF_6, 1.69	BrF_2^+, 1.69	BrF_6^-, 1.85	BrF_4^-, 1.89	KrF_2, 1.88
	SnF_3^-, 2.04	SnF_6^{2-}, 1.97				
SnF_4, 1.84	SbF_3, 1.88	SbF_6^-, 1.87				
	TeF_3^+, 1.84	TeF_6, 1.82		XeF_6, 1.89	XeF_4, 1.94	XeF_2, 1.98

Recent references to be noted: AF_3^+ [99,100], SnF_3^- [101], BrF_4^-, BrF_6^- [102], XeF_4 [103].

reactions of the types $AX_k \rightarrow AX_{k-1} + X^-$ and $AX_k + A'X_{k'} \rightarrow AX_{k'} + A'K_k$ occurring with a decrease in η (see Fig. 7).

F. ANALYSIS OF THE BEHAVIOUR OF LONE PAIR ELECTRONS IN TERMS OF CANONICAL MOLECULAR ORBITALS

The separation of the charge density derived from lone pair (LP) electrons from that for bond pairs (BPs) provides the basis for the Gillespie–Nyholm theory and is unambiguously established [10–16]. The greater size of the LP compared with that of the BP has been demonstrated [14,15] by studies of the charge density Laplacian for a considerable number of typical molecules. This is used to describe the characteristic distortion in the geometry of such molecules, e.g. the deviation of equatorial ligands towards the axial ligand in SbX_5^{2-}, IF_5, XeF_5^+, and in other valence-isoelectron compounds with a tetragonal-pyramidal structure, or decrease in bond angles in molecules such as SF_4, ClF_3, etc. compared with the values characteristic of the trigonal-bipyramidal structures.

However, we believe that it is also possible to analyse the LP behaviour within the canonical MO framework in terms of the Berlin–Bader diagrams [64–66]. Such an analysis will be of equal usefulness for the comparative assessment of the stereochemical activity of LPs in various molecular shapes and for a comparative study of the AX_k^p halides with different X.

TABLE 11

Correlation between hypervalence index, η, and bond length (Å)

AX_4, T_d 1.00	AX_3, C_{3v} 1.14	AX_6, O_h 1.20	AX_2, C_{2v} 1.33	AX_6, $C_{ av}$–O_h 1.40	AX_4, D_{4h} 1.50	AX_2, $D_{\infty h}$ 1.66
$AlCl_4^-$, 2.13						
$SiCl_4$, 2.02	PCl_3, 2.04	PCl_6^-, 2.06				
PCl_4^+, 1.91	SCl_3^+, 1.97		SCl_2, 2.01			
$GaCl_4^-$, 2.17	$GeCl_3^-$, 2.27	$GeCl_6^{2-}$, 2.35				
$GeCl_4$, 2.11	$AsCl_3$, 2.16		$SeCl_2$, 2.16	$SeCl_6^{2-}$, 2.40		$BrCl_2^-$, 2.37
	$SeCl_3^+$, 2.10					
$InCl_4^-$, 2.33	$SnCl_3^-$, 2.52	$SnCl_6^{2-}$, 2.42				
$SnCl_4$, 2.28	$SbCl_3$, 2.33	$SbCl_6^-$, 2.36		$SbCl_6^{3-}$, 2.65		ICl_2^-, 2.55
$SbCl_4^+$, 2.22	$TeCl_3^+$, 2.26		$TeCl_2$, 2.33	$TeCl_6^{2-}$, 2.54	$TeCl_4^{2-}$, 2.61	
$PbCl_4$, 2.43	$BiCl_3$, 2.48			$BiCl_6^{3-}$, 2.66		
$SiBr_4$, 2.15	PBr_3, 2.22					
PBr_4^+, 2.15	SBr_3^+, 2.14					

$GeBr_4$, 2.27	$AsBr_3$, 2.33 $SeBr_3^+$, 2.27		$SeBr_6^{2-}$, 2.58	$SeBr_4^{2-}$, 2.60	Br_3^-, 2.55
$InBr_4^-$, 2.50 $SnBr_4$, 2.44	$SbBr_3$, 2.49 $TeBr_3^+$, 2.43	$SbBr_6^-$, 2.56	$SbBr_6^{3-}$, 2.79 $TeBr_6^{2-}$, 2.70	$TeBr_4^{2-}$, 2.75	IBr_2^-, 2.71
	$BiBr_3$, 2.63		$BiBr_6^{3-}$, 2.84		
	PI_3, 2.46				
GeI_4, 2.50	SeI_3^+, 2.51 AsI_3, 2.56				
SnI_4, 2.64	TeI_3^+, 2.66 SbI_3, 2.72		TeI_6^{2-}, 2.93	TeI_4^{2-}, 2.98	I_3^-, 2.93
			BiI_6^{3-}, 3.07		

Recent references to be noted: AX_3^+ [99,100], AY_6^{n-} [79,104(a)], AY_4^{2-} [104(b)]; other bond lengths from refs. 5, 28 and 63.

TABLE 12

Correlation between hypervalence index, η, and bond length (Å) in compounds AX_k with non-equivalent bonds

AX_k, symm. η	AX_5, D_{3h} 1.11	AX_4, C_{2v} 1.25	AX_5, C_{4v} 1.33	AX_3, C_{2v} 1.44
R	1.58	1.64	1.67	1.70
	PF_5	SF_4	ClF_5	ClF_3
R′	1.53	1.54	1.57	1.60
R	1.65			
	SiF_5^-			
R′	1.59			
R	1.71	1.77	1.77	1.81
	AsF_5	SeF_4	BrF_5	BrF_3
R′	1.66	1.68	1.69	1.72
R		1.90	1.87	
		TeF_4	IF_5	
R′		1.79	1.83	
R		1.83	1.86	1.91
		IF_4^+	XeF_5^+	XeF_3^+
R′		1.79	1.78	1.84
R		2.04	1.95	
		SbF_4^-	TeF_5^-	
R′		1.93	1.86	
R			2.08	
			SbF_5^{2-}	
R′			1.97	
R	2.13			
	PCl_5			
R′	2.02			
R			2.36	
			$SeCl_5^-$	
R′			2.16	
R	2.34	2.76	2.65	
	$SbCl_5$	$SnCl_4^{2-}$	$SbCl_5^{2-}$	
R′	2.29	2.51	2.36	

Recent communications: ClF_3 [105], SiF_5^- [106], AsF_5 [107], SbF_4^- [108], $SeCl_5^-$ [109], $SnCl_4^{2-}$ [110]; other data from refs. 5, 28, 63 and 91.

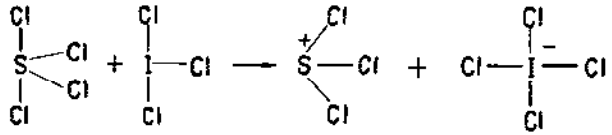

$$TeF_4 \longrightarrow TeF_3^+ + F^-$$
$$\eta = 1.25 \qquad \eta = 1.14$$

$$XeF_6 \longrightarrow XeF_5^+ + F^-$$
$$\eta = 1.40 \qquad \eta = 1.33$$

Fig. 7. Some examples of relationships between hypervalence index and direction of chemical transformations for AX_k systems.

Firstly, we should note the possibility of applying the hypervalence index η for an analysis of LP dimensions in the series $AX_k^{\prime}$ ($k = 3$–5). We can assume that the volume of the electronic density pushed out from the bond region grows with the number of electrons per AO participating in the bonding. Thus, a growth of η in a series AF_3 (C_{3v}, 1.14), AF_4 (C_{2v}, 1.25), and AF_5 (C_{4v}, 1.33) suggests an increase in the LP size, and hence in their stereochemical activity, in agreement [97] with the observed deviation of the bond angles from the values for those in corresponding polyhedra: tetrahedron, trigonal bipyramid, and tetragonal pyramid.

The possibility of analysis, within the canonical MO framework, of more subtle effects related to variations in the stereochemical activity of LPs will be demonstrated for the SbX_5^{2-} anions (X = F, Cl). We shall consider the following main factors which should affect the distortions mentioned above of the tetragonal pyramid:

(1) Increase in the overlap between σ-orbitals of the equatorial ligands and p_z-AO of the central atom (this overlap is equal to zero in a regular pyramid).

(2) Decrease in the overlap of these ligand orbitals with the p_x- and p_y-AOs of the central atom (in a regular pyramid this overlap reaches a maximum).

(3) Repulsion of the Sb–X equatorial bonds from LPs measured by a change of the negative overlap between Sb 5s-AO and σ-orbitals of the equatorial ligands.

(4) Repulsion of equatorial ligands from the axial ligand, which can be evaluated by the negative overlap population of the corresponding ligands.

As can easily be seen, effects due to the first and second factors will essentially compensate each other because the increase in the overlap of σ-AOs of the equatorial ligands with the p_z-AO of the central atom in the a_1 MO is approximately equal to the decrease in the ovelap of the ligand σ-AOs with the central atom p_x- and p_y-AOs in the e MO. For this reason, major attention will be given to the analysis of the last two factors. The possibility of charge density accumulation in the form of

LPs at the Sb atom on the side opposite to the axial ligand in SbX_5^{2-} has been argued against in some reports [111–113].

The negative sign of the overlap population of the Sb 5s-AO and the equatorial ligand σ-AOs upon summation over the occupied MOs in the a_1 representation of the SbX_5^{2-} systems (see Table 13) shows evidence for charge density accumulation outside the bond region, in accordance with the Berlin diagram. Here and in what follows the analysis is based on the calculations of ref. 112. Comparison between the $\Sigma_{MO_s}^{occ} P(5s\text{-}\sigma)$ for the $SbCl_5^{2-}$ systems with the Cl_aSbCl_e angles of 85° and 95° shows a greater "repulsion by the LP" in the latter case. The chlorine 3s-AOs also produce an antibonding contribution to the Sb–Cl_e interaction, and hence lead to an increase in the "LP size" and in the repulsion of the Sb–Cl_e bonds from the LP.

It would be of interest to compare the overlap populations of the Sb 5s-AO with the ligand AOs in $SbCl_5^{2-}$ and SbF_5^{2-} in order to estimate the relative "stereochemical activity" of LPs. The data presented in Table 13 show the "repulsion of the Sb–X equatorial bonds from the LP" in SbF_5^{2-} to be reduced compared with that in $SbCl_5^{2-}$. This is also supported by a greater population of the 5s-AO in $SbCl_5^{2-}$ in both the distorted structures and the regular pyramid [112]. Thus, the question arises of why the X_aSbX_e angle in SbF_5^{2-} is smaller (and hence the deviation of equatorial ligands greater) than that in $SbCl_5^{2-}$. A comparison of the X_a–X_e overlap populations for these two systems provides an explanation, showing that, even for a smaller X_aSbX_e angle in SbF_5^{2-}, a negative $P(X_a\text{–}X_e)$ value in SbF_5^{2-} is smaller than that in $SbCl_5^{2-}$. Thus, repulsion from the LP takes place in SbX_5^{2-} compounds while the magnitude of the ligand deviation is considerably affected by repulsion of the ligands.

In addition, we note another feature that distinguishes pentafluoro anions from pentachloro anions: a considerably larger contribution of P(5s-2s) to the Sb–F overlap population compared with that of P(5s-3s) to the corresponding P(Sb–Cl) value. This is a characteristic feature of first row non-transition elements which is accounted for by the close dimensions of the 2s- and 2p-AOs and a greater difference in the radii of the Cl 3s- and 3p-AOs [46].

TABLE 13

Overlap populations (P) of 5s-AO Sb with s_X- and σ_X-AOs, populations (q) 5s-AO Sb and $P(X_a \cdots X_e)$ for SbX_5^{2-}

SbX_5^{2-} ($\angle X_aSbX_e$)	$SbCl_5^{2-}$ (95°)	$SbCl_5^{2-}$ (85°)	SbF_5^{2-} (80°)	SbF_5^{2-} (90°)
$\sum^{occ} P(5s\text{-}\sigma_e)$	−0.086	−0.050	−0.002	−0.024
$\sum^{occ} P(5s\text{-}s_e)$	−0.032	−0.028	−0.022	−0.028
q(5s)	1.784	1.768	1.564	1.601
$P(X_a \cdots X_e)$	−0.034	−0.066	−0.040	−0.016

G. CONCLUSION

Using the main group halides as an example, we have demonstrated the possibility of analysing molecular geometry within the MO framework, including even those aspects which have so far been predominantly within the scope of the VSEPR model: the description of molecular shapes and lone pair electrons. At least, we find it useful to treat these problems from different points of view.

In the present review, we have restricted consideration to halides, mostly of the AX_k^p type, because they present a convenient subject to demonstrate both the action of the rule of non-occupation of the maximally antibonding MOs and the possible application of the hypervalence index η. The rule of MAMO non-occupation relates only to the symmetry of the system considered and requires no modification when applied to other AX_k^p compounds with non-halogen ligands. The use of η in the case of other ligands, however, will demand some changes in the determination of the number of electrons participating in bonding, e.g. by assuming that no ligand electrons are involved in the case of group VI elements as ligands (oxygen in SO_4^{2-}, ClO_2^-, etc.).

We have intentionally omitted consideration of problems related to the AX_lY_{k-l} molecules. On the one hand, they have been exhaustively discussed by Levin and Dyachkov [114]. On the other hand, treatment of these compounds within the framework of our approach would require special consideration for the effects of electronegativity of atoms forming the AX_lY_{k-l} molecules on the nodal properties of MOs, and the application of the concept of charge distribution topology. These aspects of chemical bonding have been extensively developed in recent years [115–119].

We emphasize that the application of η to a comparative study of chemical bonds is not restricted to bond lengths. One example, already mentioned above, concerns the transformation of compounds to products with lower η compared with the initial species. Many AX_k^p compounds can be included in a possible correlation of η with force constants (or vibrational frequencies) of the A–X bonds.

ACKNOWLEDGEMENTS

We thank Prof. R.J Gillespie for helpful and stimulating discussion, and Dr. G.L. Gutsev for critically reading the manuscript and valuable comments.

REFERENCES

1 W.J. Hehre, L. Radom, P.v.R. Schleyer and J.A. Pople, Ab initio Molecular Orbital Theory, Wiley, New York, 1986.
2 A. Hinchliffe, Ab initio Determination of Molecular Properties, Hilger, Bristol, 1987.
3 Quantum Chemistry Literature Data Base, Supplement 9. Bibliogtaphy of Ab initio

Calculations for 1989. K. Ohno, K. Morokuma and H. Hosoya (Eds.), J. Mol. Struct., 211 (1990) 1, and references cited therein.
4 J.P. Lowe, Quantum Chemistry, Academic Press, New York, 1979.
5 B.M. Gimarc, Molecular Structure and Bonding: The Qualitative MO Approach, Academic Press, New York, 1979.
6 J.K. Burdett, Molecular Shapes. Theoretical Models of Inorganic Stereochemistry, Wiley, New York, 1985.
7 R.G. Buenker and S.D. Peyrimhoff, Chem. Rev., 74 (1974) 955.
8 T.A. Albright, J.K. Burdett and M.H. Whangbo, Orbital Interactions in Chemistry, Wiley, New York, 1985.
9 (a) R.J. Gillespie, Molecular Geometry, Van Nostrand Reinhold, London, 1972.
(b) R.J. Gillespie and I. Hargittai, The VSEPR Model of Molecular Geometry, Allyn and Bacon, London, 1991.
10 R.F. Ziolo and M. Troup, J. Am. Chem. Soc., 105 (1983) 229.
11 I.P. Makarova, L.A. Muradyan, V.E. Zavodnik and V.I. Simonov, Dokl. Akad. Nauk SSSR, 283 (1985) 126.
12 M.Yu. Antipin, A.M. Ellern, V.F. Sukhoverkhov, Yu.T. Struchkov and Yu.A. Buslaev, Dokl. Akad. Nauk SSSR, 293 (1987) 1152.
13 L. Mensching, W. Von Niessen, P. Valtazanos, K. Ruedenberg and W.H.E. Schwarz, J. Am. Chem. Soc., 111 (1989) 6933.
14 R.F.W. Bader, P.J. MacDougall and C.D. Lau, J. Am. Chem. Soc., 106 (1984) 1594.
15 (a) R.F.W. Bader, R.J. Gillespie and P.J. MacDougall, J. Am. Chem. Soc., 110 (1988) 7329.
(b) R.F.W. Bader, R.J. Gillespie and P.J. MacDougall, in J.F. Liebman and A. Greenberg (Eds.), Molecular Structures and Energetics, Vol. 11, VCH Publishers, New York, 1989, Chap. 1.
(c) R.F.W. Bader, Atoms in Molecules: A Quantum Theory, Oxford University Press, Oxford, 1990.
16 A.D. Becke and R.E. Edgecombe, J. Chem. Phys., 92 (1990) 5397.
17 V.G. Tsirelson and M.Yu. Antipin, in M.A. Porai-Koshits (Ed.), Problems of Crystal Chemistry, Nauka, Moscow, 1989, p. 119 (in Russian).
18 D. Cremer, in L.B. Maksic (Ed.), Modeling of Structure and Properties of Molecules, Ellis Horwood, Chichester, 1987, p. 125.
19 R.S. Mulliken, Rev. Mod. Phys., 14 (1942) 204.
20 A.D. Walsh, J. Chem. Soc., (1953) 2260, 2266, 2296, 2301.
21 P. Siddarth and M.S. Gopinatham, J. Am. Chem. Soc., 110 (1988) 96.
22 L.C. Allen, Theor. Chim. Acta, 24 (1972) 117.
23 L.S. Bartell and V. Plato, J. Am. Chem. Soc., 95 (1973) 3097.
24 A.P. Klyagina, Koord. Khim., 3 (1977) 955.
25 F.A. Cotton and R.A. Walton, Multiple Bonds between Metal Atoms, Wiley, New York, 1982, Chap. 8.
26 S.W. Ng and J.J. Zuckerman, Adv. Inorg. Chem. Radiochem., 29 (1985) 297.
27 L.M. Volkova and A.A. Udovenko, in M.A. Porai-Koshits (Ed.), Problems of Crystal Chemistry, Nauka, Moscow, 1987, p. 46 (in Russian).
28 M. Hargittai, Coord. Chem. Rev., 91 (1988) 35.
29 D.M.P. Mingos and J.C. Hawes, Struct. Bonding (Berlin), 63 (1985) 1.
30 P.K. Mehrotra and R. Hoffmann, Theor. Chim. Acta, 48 (1978) 301.
31 A.P. Klyagina and M.E. Dyatkina, Zh. Strukt. Khim., 14 (1972) 908.
32 H.H. Schmidtke, Int. J. Quantum Chem., 7 (1973) 127.

33 E.B. Wilson, J. Chem. Phys., 63 (1975) 4870.
34 J.K. Burdett, in R.B. King and D.H. Rouvray (Eds.), Graph Theory and Topology in Chemistry, Elsevier, Amsterdam, 1987, p. 302.
35 M.E. Dyatkina and N.M. Klimenko, Zh. Strukt. Khim., 14 (1973) 174.
36 K.A.R. Mitchel, Chem. Rev., 69 (1969) 157.
37 C.A. Coulson, Nature, 211 (1969) 221, 1106.
38 D.A. Bochvar, N.P. Gambaryan and L.M. Apstein, Usp. Khim., 45 (1976) 1316.
39 G.L. Gutsev and A.P. Klyagina, Chem. Phys., 75 (1983) 243.
40 A.P. Klyagina, G.L. Gutsev and A.A. Levin, Zh. Neorgan. Khim., 29 (1984) 1442.
41 S. Xiao, W.C. Trogler, D.E. Ellis and L. Berkovitch-Yellin, J. Am. Chem. Soc., 105 (1983) 7033.
42 D.S. Marynick, J. Am. Chem. Soc., 106 (1984) 4064.
43 M. Braga, Inorg. Chem., 24 (1985) 2702.
44 L.S. Barteli, M.J. Rothman and A. Gavezzotti, J. Chem. Phys., 76 (1982) 4136.
45 M. Grodicki and S. Elbel, in L.B. Maksic (Ed.), Modeling of Structure and Properties of Molecules, Ellis Horwood, Chichester, 1987, p. 239.
46 W. Kutzelnigg, Angew. Chem. Int. Ed. Engl., 23 (1984) 272.
47 A.E. Reed and F. Weinhold, J. Am. Chem. Soc., 108 (1986) 3586.
48 A.E. Reed and P.v.R. Schleyer, J. Am. Chem. Soc., 112 (1990) 1434.
49 C.H. Patterson and R.P. Messmer, J. Am. Chem. Soc., 112 (1990) 4138.
50 R.F. Hout, W.J. Pietro and W.J. Hehre, A Pictorial Approach to Molecular Structure and Reactivity, Wiley, New York, 1984.
51 K.M. Mackay and R.A. Mackay, Introduction to Modern Inorganic Chemistry, Blackie, Glasgow, 4th edn., 1989.
52 J.K. Burdett and C.J. Marsden, New J. Chem., 12 (1989) 797.
53 P. Pyykko, Chem. Rev., 88 (1988) 563.
54 P. Pyykko and P. Desclaux, Acc. Chem. Res., 12 (1979) 276.
55 K.S. Pitzer, Acc. Chem. Res., 12 (1979) 271.
56 K. Balasubramanian and K.S. Pitzer, Adv. Chem. Phys., 67 (1987) 287.
57 J.I. Musher, Angew. Chem. Int. Ed. Engl., 8 (1969) 54.
58 R.E. Rundle, Rec. Chem. Prog., 23 (1962) 195.
59 R.E. Rundle, Surv. Prog. Chem., 1 (1963) 81.
60 K.S. Pitzer, Science, 139 (1963) 414.
61 L.M. Babcock and G.E. Streit, J. Chem. Phys., 75 (1981) 3865.
62 T. Kiang and R.N. Zare, J. Am. Chem. Soc., 102 (1980) 4024.
63 A.F. Wells, Structural Inorganic Chemistry, Clarendon Press, Oxford, 5th edn., 1986.
64 T. Berlin, J. Chem. Phys., 19 (1951) 208.
65 R.F.W. Bader, J. Am. Chem. Soc., 86 (1964) 5070.
66 R.F.W. Bader, in B.M. Deb (Ed.), The Force Concept in Chemistry, van Nostrand, New York, 1981, p. 33.
67 L. Pauling, The Nature of the Chemical Bond and the Structure of Molecules and Crystals, Cornel University Press, Ithaca, New York, 3rd edn., 1960.
68 E.A. Magnusson, Int. Rev. Chem., 5 (1986) 147.
69 E.A. Magnusson and H.F. Schaefer, J. Chem. Phys., 83 (1985) 5721.
70 A. Engelbrecht and F. Sladky, Adv. Inorg. Chem. Radiochem., 24 (1981) 211.
71 M.A. Ratner and J.R. Sabin, J. Am. Chem. Soc., 99 (1977) 3954.
72 I.B. Bersuker, A.S. Deemoglo and A.A. Levin, in M.G. Veselov (Ed.), Recent Problems in Quantum Chemistry, Nauka, Leningrad, 1986, p. 102.
73 W.R. Rodwell, J. Am. Chem. Soc., 100 (1978) 7209.

74 A.P. Klyagina, A.A. Levin and G.L. Gutsev, Chem. Phys. Lett., 77 (1981) 365.
75 H. Adachi, J. Electron Spectrosc. Relat. Phenom., 16 (1979) 277.
76 A.P. Klyagina, G.L. Gutsev, V.D. Fursova and A.A. Levin, Zh. Neorgan. Khim., 29 (1984) 2765.
77 C.S. Ewig and J.R. Van Wazer, J. Am. Chem. Soc., 111 (1989) 4172.
78 (a) K.O. Christie and W.W. Wilson, Inorg. Chem., 28 (1989) 3275.
(b) K. Seppelt, Comments Inorg. Chem., 12 (1991) 199.
79 A. Du Bois and W. Abriel, Z. Naturforsch. Teil B, 43 (1988) 1003.
80 M. Spoliti, G. De Maria, L.D. Alessio and M. Maltese, J. Mol. Struct., 67 (1980) 159.
81 F. Ramondo, V. Rossi and L. Bencivenni, Mol. Phys., 64 (1988) 513.
82 (a) R.L. Dekock, M.A. Peterson, L.K. Timmer, E.J. Baerends and P. Vernooiys, Polyhedron, 9 (1990) 1919.
(b) L. Seito, Z. Barandiaran, S. Huzinaga, J. Chem. Phys., 94 (1991) 3762.
(c) M. Kaupp, P.V.R. Schleyer, H. Stoll and H. Preuss, J. Am. Chem. Soc., 113 (1991) 6012.
83 E.F. Hayes, J. Phys. Chem., 70 (1966) 3740.
84 N.M. Klimenko, D.G. Musaev and O.P. Charkin, Zh. Neorgan. Khim., 29 (1984) 1114.
85 J.M. Dyke and T.G. Wright, Chem. Phys. Lett., 169 (1990) 138.
86 D.M. Hassett and C.J. Marsden, J. Chem. Soc. Chem. Commun., (1990) 667.
87 U. Salzner and P.v.R. Schleyer, Chem. Phys. Lett., 172 (1990) 461.
88 M. Guido and G. Gigli, J. Chem. Phys., 65 (1976) 1397.
89 M.C. Drake and G.M. Rosenblatt, J. Electrochem. Soc., 126 (1979) 1387.
90 L. von Szentpaly and P. Schwerdtfeger, Chem. Phys. Lett., 170 (1990) 555.
91 (a) J.H. Calloman, E. Hirota and T. Iijima, in H. Landolt and R. Bornstein, Zahlenwerten und Fuctionen aus Naturwissenschaften und Technik, New Series, Group 11, Vol. 15, 1987, Springer, Berlin.
(b) S. Subramanian and M.T. Rogers, J. Chem. Phys., 57 (1972) 4582.
92 (a) N.C. Baird, M. Kuhn and T.M. Laurison, Can. J. Chem., 67 (1989) 1952.
(b) M. Cattani-Lorente and M. Geoffroy, Chem. Phys. Lett., 167 (1990) 460.
93 (a) V.I. Sergienko, L.N. Ignat'eva and A.Yu. Beloliptsev, Zh. Fiz. Khim., 64 (1990) 694.
(b) T. Ziegler and G.L. Gutsev, J. Chem. Phys., 96 (1992) 7623.
(c) G.L. Gutsev, Zh. Neorgan. Khim., 37 (1992) 2160.
94 V.O. Gelmboldt and A.A. Annun, Usp. Khim., 58 (1989) 626.
95 N.P. Gambaryan and I.V. Stankevich, Usp. Khim., 58 (1989) 1945.
96 K. Lutar, A. Jesih, I. Leban, B. Lemva and N. Bartlett, Inorg. Chem., 28 (1989) 3467.
97 Yu.E. Gorbunova, Yu.V. Kokunov and Yu.A. Buslaev, Pure Appl. Chem., 59 (1989) 155.
98 M.Yu. Antipin, A.M. Ellern, V.F. Sukhoverkhov, Yu.T. Struchkov and Yu.A. Buslaev, Zh. Neorgan. Khim., 33 (1988) 307.
99 J.P. Johnson, M. Murchi, J. Passmore, M. Tajik, P.S. White and C.M. Wohg, Can. J. Chem., 65 (1987) 2744.
100 B.H. Christian, M.J. Collins, R.J. Gillespie and J.F. Sawger, Inorg. Chem., 25 (1986) 777.
101 Yu.V. Kokunov, Yu.E. Gorbunova, V.N. Petrov, M.P. Gustyakova and Yu.A. Buslaev, Dokl. Akad. Nauk SSSR, 307 (1989) 1126.
102 A.R. Mahjoub, A. Hoser, J. Fuchs and K. Seppelt, Angew. Chem. Int. Ed. Engl., 28 (1989) 1526.
103 L.S. Ivashkevich, A.A. Ishchenko, Yu.M. Kiselev, G.V. Romanov, V.B. Sokolov and V.P. Spiridonov, Dokl. Akad. Nauk SSSR, 305 (1989) 1396.
104 (a) S.C. Abrahams, J. Ihringer and P. Marsh, Acta Crystallogr. Sect. B, 45 (1989) 26.
(b) S. Pohl, W. Saak and B. Krebs, Z. Naturforsch. Teil B, 40 (1985) 251.
105 M.Yu. Antipin, A.M. Ellern, V.F. Sukhoverkhov and Yu.T. Struchkov, Zh. Neorgan. Khim., 34 (1989) 819.

106 D. Schomburg and R. Krebs, Inorg. Chem., 23 (1984) 1378.
107 J. Kohler, A. Simon and R. Hoppe, Z. Anorg. Allg. Chem., 575 (1989) 55.
108 A.A. Udovenko, R.L. Davidovich, M.Yu. Antipin and Yu.T. Struchkov, Koord. Khim., 16 (1990) 448.
109 R.J. Gillespie, J.P. Kent and J.F. Sawger, Inorg. Chem., 29 (1990) 1251.
110 V.I. Sokol, T.G. Vasilenko, M.A. Porai-Koshits, A.K. Molodkin and S.V. Vasnin, Zh. Neorgan. Khim., 35 (1990) 2017.
111 V.I. Sergienko, V.I. Kostin, L.N. Ignat'eva and G.L. Gutsev, J. Fluorine Chem., 32 (1986) 367.
112 V.I. Sergienko, G.L. Gutsev, L.N. Ignat'eva, V.I. Kostin and V.A. Davidov, Zh. Fiz. Khim., 60 (1986) 350.
113 V.I. Sergienko, L.N. Ignat'eva and T.V. Volodkina, Zh. Fiz. Khim., 63 (1989) 1256.
114 A.A. Levin and P.N. Dyachkov, Electronic Structure, Geometry, Isomerism and Transformations of Heteroligand Molecules, Nauka, Moscow, 1990 (in Russian).
115 K.D. Sen, M.C. Böhm and P.C. Schmidt, Struct. Bonding (Berlin), 66 (1987) 99.
116 R.G. Pearson, Inorg. Chem., 27 (1988) 734.
117 L.C. Allen, J. Am. Chem. Soc., 111 (1989) 9003.
118 B.M. Gimarc and J.J. Ott, in R.B. King and D.H. Rouvray (Eds.), Graph Theory and Topology in Chemistry, Elsevier, Amsterdam, 1987, p. 285.
119 K.E. Edgekombe, J. Mol. Struct. (Theochem.), 226 (1991) 157.